Computational and Structural Biotechnology Journal 20 (2022) 5911–5924

COMPUTATIONAL ANDSTRUCTURAL BIOTECHNOLOGY JOURNAL

journal homepage: www.elsevier.com/locate/csbj

Finer resolution analysis of transcriptional programming during the active migration of chicken primordial germ cells

Deivendran Rengaraj [a,1], Dong Gon Cha [b,1], Kyung Je Park [a], Kyung Youn Lee [a], Seung Je Woo [a], Jae Yong Han [a,*]

[a] Department of Agricultural Biotechnology, and Research Institute of Agriculture and Life Sciences, Seoul National University, Seoul 08826, Korea
[b] Department of New Biology, DGIST, Daegu 42988, Korea

ARTICLE INFO

Article history:
Received 7 May 2022
Received in revised form 4 October 2022
Accepted 21 October 2022
Available online 26 October 2022

Keywords:
Chicken
PGCs
Migration
Single-cell RNA sequencing
Sex differences
Transcription factors

ABSTRACT

Primordial germ cells (PGCs) in chickens polarize and move passively toward the anterior region by the morphogenetic movement of the embryo. Further migration of PGCs towards the genital ridge via the germinal crescent region and blood vessels occurs actively through the chemoattractive signals. The mechanisms of initiation of PGCs migration, lodging the PGCs in the vascular system, and colonization of PGCs in the gonads are well-studied. However, transcriptome sequencing-based cues directing the migration of the PGCs towards gonads, some of the relevant molecules, biological processes, and transcription factors (TFs) are less studied in chickens. The current study comprehensively interprets the transcriptional programming of PGCs during their active migration (E2.5 to E8). Current results revealed several vital understandings, including a set of genes that upregulated male-specifically (*XPA*, *GNG10*, *RPL17*, *RPS23*, and *NDUFS4*) or female-specifically (*HINTW*, *NIPBL*, *TERAL2*, *ATP5F1AW*, and *SMAD2W*) in migrating PGCs, and transcriptionally distinct PGCs, particularly in the gonadal environment. We identified DNA methylation and histone modification-associated genes that are novel in chicken PGCs and show a time-dependent enrichment in migrating PGCs. We further identified a large number of differentially expressed genes (DEGs, including TFs) in blood PGCs (at E2.5) compared to gonadal PGCs (at E8) in both sexes; however, this difference was greater in males. We also revealed the enriched biological processes and signaling pathways of significant DEGs identified commonly, male-specifically, or female-specifically between the PGCs isolated at E2.5, E6, and E8. Collectively, these analyses provide molecular insights into chicken PGCs during their active migration phase.

1. Introduction

Primordial germ cells (PGCs), which have an extragonadal origin, are the precursors of sperms and oocytes. After the fusion of the sperm and oocyte, the totipotent zygote has a remarkable capacity to develop into a new organism. All cells of the new organism are descendants of PGCs. Therefore, the specification of PGCs can be regarded as a crucial first step for acquiring totipotency and continuing the life cycle [1]. The specification of PGCs was reported by an epigenesis mode in mammals. In contrast, several species in the animal classes, including aves, anura, teleostei, and insecta, use the inherited mode of the PGCs specification [2]. In chicken, a best-studied species of aves, a maternally inherited component called "germ plasm" that consists of a set of RNAs, proteins, and energy-rich mitochondria are exclusively allocated to the prospective PGCs [3]. The PGCs have been detected in the central region of chicken intrauterine embryos from Eyal-Giladi and Kochav (EGK) [4] stage-III to EGK stage-X. During the post-oviposition (*in ovo*) embryonic development, PGCs migrate to the anterior region of Hamburger and Hamilton (HH) [5] stage-2 to HH stage-4. Then, the PGCs are incorporated into the semi-circular-shaped extra-embryonic region called the germinal crescent of HH stage-9 to HH stage-12. At about HH stage-13, PGCs are entered into the lumina of blood vessels and remain in blood circulation. In chickens, the vascular system serves as a vehicle to transport different cells, such as the leukocytes and PGCs, to distant locations, and migration through the vessel wall occurs in the vicinity of the target tissue [6]. The blood PGCs are entered into the future gonadal region at around HH stage-18 to HH stage-21

* Corresponding author at: Seoul National University, 1 Gwanak-ro, Gwanak-gu, Seoul 08826, Korea.
E-mail address: jaehan@snu.ac.kr (J.Y. Han).
[1] These authors contributed equally to this work.

https://doi.org/10.1016/j.csbj.2022.10.034

[3,7,8]. After entering the bilateral sexually undifferentiated gonads, gonadal PGCs undergo dynamic proliferation and differentiation in a sex-specific manner: PGCs differentiate into oogonia in females at about E8.0 and pro-spermatogonia in males at about E13.0 [9–11].

Regardless of epigenesis or inherited mode of PGCs specification, the nascent PGCs block somatic identity and maintain pluripotency. The next goal of PGCs is the migration to the gonads, where they settle down, differentiate in a sex-specific manner, and undergo a meiotic cell cycle to generate further germline cells [2]. Migrating PGCs have to overcome several hurdles as they migrate through the crowded and complex cellular environment of a developing embryo [12]. Therefore, the PGCs are provided with directional cues in the course of their migration, and also the PGCs migration in all species follows three similar steps, including initiation of polarity and directed migration, regulated migration by attractive and repulsive cues, and termination of migration in the gonads [13]. PGCs in many of the studied species, including mice, Drosophila, zebrafish, and chickens, normally use chemoattractive signals to reach the gonads [6,13,14]. Particularly in chickens and mice, genital ridge cells secrete SDF1 (a chemoattractant) that is received by PGCs transmembrane protein CXCR4 (a G protein-coupled receptor) during the course of PGCs migration [6]. Furthermore, lipids and cell adhesion molecules (such as E-cadherin and integrin β1) also play critical roles in PGCs migration [13]. Studies in chicken and quail described that the extracellular matrix (ECM) molecules such as laminin, fibronectin, chondroitin sulfate, collagen, and integrin are expressed in avian PGCs and distributed at their early migratory routes [15,16]. Thus, the PGCs interaction with the ECM molecules is important for their early migration.

Epigenetic reprogramming, including genome-wide DNA demethylation and dynamic changes in histone modifications, is a critical event in migrating PGCs. In mice, PGCs specified in the post-implantation epiblast are hypermethylated. When the PGCs start the migration, global CpG methylation levels drop significantly, and almost all genomic features become hypomethylated just before colonization in gonads. DNA methylation is then re-established in germ cells after colonization in gonads; however, in a sex-specific manner [1]. The gonadal PGCs of chicken also showed an increase in CpG methylation level [17]. Interestingly, hypomethylated migrating PGCs in humans, mice, and chickens remain proliferative and maintain the expression of critical pluripotency- and germness-specific genes [7,18,19]. Besides, activating certain signaling pathways, particularly the Wnt-signaling and TGFβ-signaling pathways, are essential for PGCs migration, proliferation, and self-renewal [20–22]. In summary, several studies in chickens have uncovered the mechanisms involved in initiating PGCs migration, lodging of the PGCs in the vascular system, and colonization of PGCs in the gonads [6,15,23]. However, transcriptome sequencing-based cues directing the migration of the PGCs towards gonads, some of the relevant molecules, biological processes, and transcription factors (TFs) are less revealed in chickens.

In our recent work, we produced a germ cell tracing model chicken by tagging of deleted in azoospermia like (*DAZL*) gene with green fluorescent protein (GFP) expression cassette (*DAZL::GFP* chickens) using CRISPR/Cas9-NHEJ-mediated genome editing. Next, the male and female germ cells from the *DAZL::GFP* chickens were isolated at embryonic day 2.5 (E2.5) to 1 week post-hatch, and the chicken germ cell dynamics were investigated by single-cell RNA sequencing (scRNA-seq) [24]. A part of the same scRNA-seq dataset (E2.5 to E8) was comprehensively investigated in the current study to interpret the transcriptional programming of PGCs during their active migration time points. We particularly defined the sex-specifically upregulated genes in migrating PGCs, transcriptionally distinct PGCs in gonads, the expression of genes associated with DNA methylation and histone modification programs of migrating PGCs, and differentially expressed genes (DEGs, including TFs) and their enriched biological processes and signaling between blood PGCs and gonadal PGCs.

2. Materials and methods

2.1. Animals

The management and experimental use of White Leghorn (WL) chickens were approved by the Institute of Laboratory Animal Resources, Seoul National University (SNU-190401–1-1). The experimental animals were cared according to a standard management program at the University Animal Farm, Seoul National University, Korea. The procedures for animal management, reproduction, and embryo manipulation adhered to the standard operating protocols of Animal Genetic Engineering Laboratory, Seoul National University.

2.2. Preparation of samples for scRNA-seq

Recently, we produced a germ cell tracing (*DAZL::GFP*) model chicken by CRISPR/Cas9-NHEJ-mediated genome editing in PGCs [24]. Briefly, the WL PGCs were maintained on knockout DMEM supplemented with essential components optimized for PGCs culture in an incubator at 37 °C with 5 % CO_2 and 60–70 % relative humidity. Cells were sub-cultured onto mitomycin-inactivated mouse embryonic fibroblasts at 5–6 day intervals [25]. We constructed two plasmids to edit chicken PGCs: donor plasmids contain the last intron and exon of *DAZL* (including the gRNA-recognition sequence) in frame with a T2A peptide and GFP expression cassette; and CRISPR/Cas9 plasmids targeting the last intron of chicken *DAZL*. Then, 2 μg of each donor and CRISPR/Cas9 plasmids were co-transfected into 1×10^5 cultured PGCs with Lipofectamine 2000 reagent. After 1 day of the transfection, G418 (300 μg/mL) was added to the culture medium to select transfected PGCs. Next, over 3,000 *DAZL* gene-edited PGCs were transplanted into the dorsal aorta of the Korean-Ogye-recipient embryo (at HH stage 14–17). After sealing the egg window with parafilm, the egg was incubated until hatching. After hatching and sexual maturation, sperm from male recipient chickens were evaluated by breed-specific PCR, and the male recipient chickens with WL sperm were mated with wild-type WL females. Germline-chimeric chickens were identified by offspring feather color and by genomic DNA analysis.

For scRNA-seq, germ cells of *DAZL::GFP* chicken embryos were collected from blood (at E2.5) and gonads (at E6 and E8). For the collection of male germ cells, we used 50–100, 35, and 11 embryos at E2.5, E6, and E8, respectively. For the collection of female germ cells, we used 50–100, 30, and 5 embryos at E2.5, E6, and E8, respectively. These embryos are G2 progeny, which includes siblings as well as from different litters. Moreover, the sex of E2.5, E6, and E8 embryos were determined by amplifying the DNA samples of embryonic blood (at E2.5) using forward (5′-CTA TGC CTA CCA CAT TCC TAT TTG C-3′) and reverse (5′-AGC TGG ACT TCA GAC CAT CTT CT-3′) primer of chicken W chromosome. The pooled blood or gonad samples from each sex and stage were treated with Hank's Balanced Salt Solution (Gibco Invitrogen, Grand Island, NY, USA) containing 0.05 % trypsin–EDTA (Gibco Invitrogen) and incubated at 37 ℃ for 10 min. Then, trypsin–EDTA was inactivated by adding an equal volume of DMEM containing 5 % fetal bovine serum (FBS; Hyclone, Logan, UT, USA). Cells were harvested by centrifugation at 1,250 rpm for 5 min, washed with PBS, resuspended in PBS containing 1 % bovine serum albumin (BSA), and filtered through a 40-μm cell strainer (Fisher Scientific, Hampton, NH, USA). Finally, cells were stained with propidium iodide (PI), and GFP^+/PI^- live cells were sorted by using a BD fluorescence-

activated cell sorting (FACS) Aria III (BD Biosciences, San Jose, CA, USA). The number of GFP^+/PI^- live cells isolated by FACS was: 500 at E2.5, 1666 at E6, and 2577 at E8 in males; 1000 at E2.5, 2253 at E6, and 4623 at E8 in females.

2.3. scRNA-seq and data preprocessing

Libraries for scRNA-seq were prepared using the Chromium Single Cell 3′ *GEM*, Library & Gel Bead Kit v3; Chromium Single Cell B Chip Kit; and Chromium i7 Multiplex Kit (10X Genomics, Pleasanton, CA, USA). Libraries were sequenced with a 2 × 100-bp paired-end protocol on a Novaseq-6000 platform to generate at least 40,000 read pairs per cell [24]. The CellRanger pipeline was used to process raw fastq files. The *DAZL-GFP* insert sequence was included to the fasta and GTF GRCg6a.99 files for the chicken genome (GRCg6a). STAR aligner [26] was used to map the cDNA sequences to the modified-chicken genome. Using the default parameters, a gene-by-cell count matrix was created. The EmptyDrops function of the DropletUtils R package [27] was used with FDR 0.05 to remove empty droplets while capturing single cells. Low-quality cells were eliminated by employing various cutoff thresholds for each sample. Using the calculateQCMetrics function of the scater R package [28], the cutoff criteria were determined by visually inspecting outliers in the principal component analysis (PCA) plot on the quality-control metrics. Cells with<3.5, 3.5, and 4.0 total log10-scaled unique molecular identifier (UMI) count with>10, 10, and 15 % of UMIs assigned to mitochondrial genes were excluded from E2.5, E6, and E8 samples, respectively. Cells were grouped using the quickCluster function of scran R package [29] to remove cell-specific biases. The computeSumFactors function in the same package was used with default parameters to calculate cell-specific size factors. The raw UMI counts were divided by cell-specific size factors to normalize the gene-by-cell count matrix of the E2.5 sample. The normalized counts were then log2-transformed by adding a pseudo-count of 1. Using the scran package's decomposeVar and getTopHVGs functions, a thousand highly variable genes (HVGs) in E2.5 PGCs were chosen based on biological variability. On the first 15 principal components (PCs), the *k*-nearest neighbor (kNN) graph was constructed using the FindNeighbors function of the Seurat R package [30], and the FindClusters function with resolution = 1.0 was used to compute clusters. RunUMAP function of the same package was used to calculate uniform manifold approximation and projection (UMAP) on the 15 PCs. The signature scores of the W-chromosome genes were calculated for the remaining clusters, and those with positive values were labeled as female PGCs, while those with negative scores were labeled as male PGCs. Count matrices of the samples (E2.5–E8) for each sex were aggregated. Further normalization, HVG selection, dimensionality reduction, and clustering were performed as described above, with 15 PCs of 750 HVGs for the count matrix and resolution = 0.8 for both males and females.

2.4. scRNA-seq data analysis of chicken PGCs

DEGs between the male and female PGCs at different time points (male versus female at E2.5, male versus female at E6, male versus female at E8) were calculated using the FindAllMarkers function of the Seurat R package. To specify enriched biological processes of these DEGs, significantly enriched gene ontology biological processes (GOBP) terms ($P < 0.05$) were selected using the topGO R package with the org.Gg.eg.db annotation data package. Significantly enriched kyoto encyclopedia of genes and genomes (KEGG) pathways ($P < 0.05$) were also selected using the KEGGREST R package [31,32]. The cell cycle of PGCs was inferred using the CellCycleScoring function of the Seurat R package, with homologous genes of mouse S phase and G2/M phase. Cells that do not express S phase or G2/M phase gene sets were auto-marked as G1 phase. DEGs of each cluster were calculated using the FindAllMarkers function of the Seurat R package. Developmental trajectories of the chicken PGCs were estimated using the Monocle3 R package [33]. UMAP was computed by using the reduce_dimension function of the package, with the first 7 PCs for both males and females. Distinct clusters were identified using the cluster_cells function of the package with resolution = 0.05 for males and 0.01 for females. Starting cells for calculating pseudotime were defined by choosing the cell with the lowest expression of POU domain class 5 transcription factor 3 (*Pou5f3*) for both male and female germ cells. Two starting cells were selected for female germ cells (E2.5 cells and E6/E8 cells), as E2.5 had a considerable distance from E6/E8.

To investigate the epigenetic reprogramming in PGCs, the complete list of chicken genes associated with the AmiGO terms such as DNA demethylation (GO:0080111) / DNA methylation (GO:0006306) and histone demethylation (GO:0016577) / histone methylation (GO:0016571) were first retrieved from the AmiGO 2 database [34,35]. The gene list was normalized by excluding overlapping annotation classes and labels, and then the average expression of genes in each category was z-scaled and visualized through mirror heatmaps. DEGs between the PGCs from different embryonic stages (E2.5 versus E6, E2.5 versus E8, and E6 versus E8) in males and females were calculated using the FindAllMarkers function of the Seurat R package. We set the cutoff values of $P < 0.05$ and logFC > 0.5 for significantly upregulated genes, and $P < 0.05$ and logFC < -0.5 for significantly downregulated genes. The expression of DEGs between the embryonic stages in male and female were visualized through heatmaps at the single-cell level. To specify enriched biological processes of significant DEGs, significantly enriched GOBP terms ($P < 0.05$) were selected using the topGO R package with the org.Gg.eg.db annotation data package. Significantly enriched KEGG pathways ($P < 0.05$) were also selected using the KEGGREST R package. Significantly upregulated and downregulated TFs in DEGs were identified by mapping the DEGs with the *Gallus gallus* TF list downloaded from the AnimalTFDB3.0 [36].

3. Results

3.1. scRNA-seq reveals a precise timing of PGCs migration

Our recent work produced a germ cell tracing (*DAZL::GFP*) model chicken by CRISPR/Cas9-NHEJ-mediated genome editing in PGCs and subsequent germline transmission. The GFP^+ and PI^- *DAZL::GFP* germ cells were isolated during the embryogenesis of male and female chickens (from blood circulation at E2.5; from gonads at E6, E8, E12, E16, hatch, and 1 week post-hatch), and studied by scRNA-seq [24]. To define the precise timing of PGCs migration at single-cell resolution, which is also necessary for the present study, we examined the expression of candidate general germ cell markers (*DAZL*, *DDX4*, and *PIWIL1*), migrating germ cell markers (*CXCR4* and *KIT*), and early/mitotic germ cell marker (*Pou5f3*) (Fig. 1). As a result of the expression patterns of *CXCR4*, a crucial chemokine receptor, the male germ cells showed higher migratory activity at E2.5 to E12, and then showed a notably decreasing trend in migratory activity. The female germ cells showed higher migratory activity at E2.5 to E8, and then their migratory activity decreased notably. The expression patterns of *KIT*, a crucial cytokine receptor, correlated with the expression of *CXCR4* in females but not males. Moreover, the migratory activities of male and female germ cells highly corresponded to their mitotic activities according to the expression patterns of *Pou5f3*. The chicken PGCs circulating in the blood enter gonadal ridges at about E3 to 3.5. However, differentiation of PGCs into oogonia in females

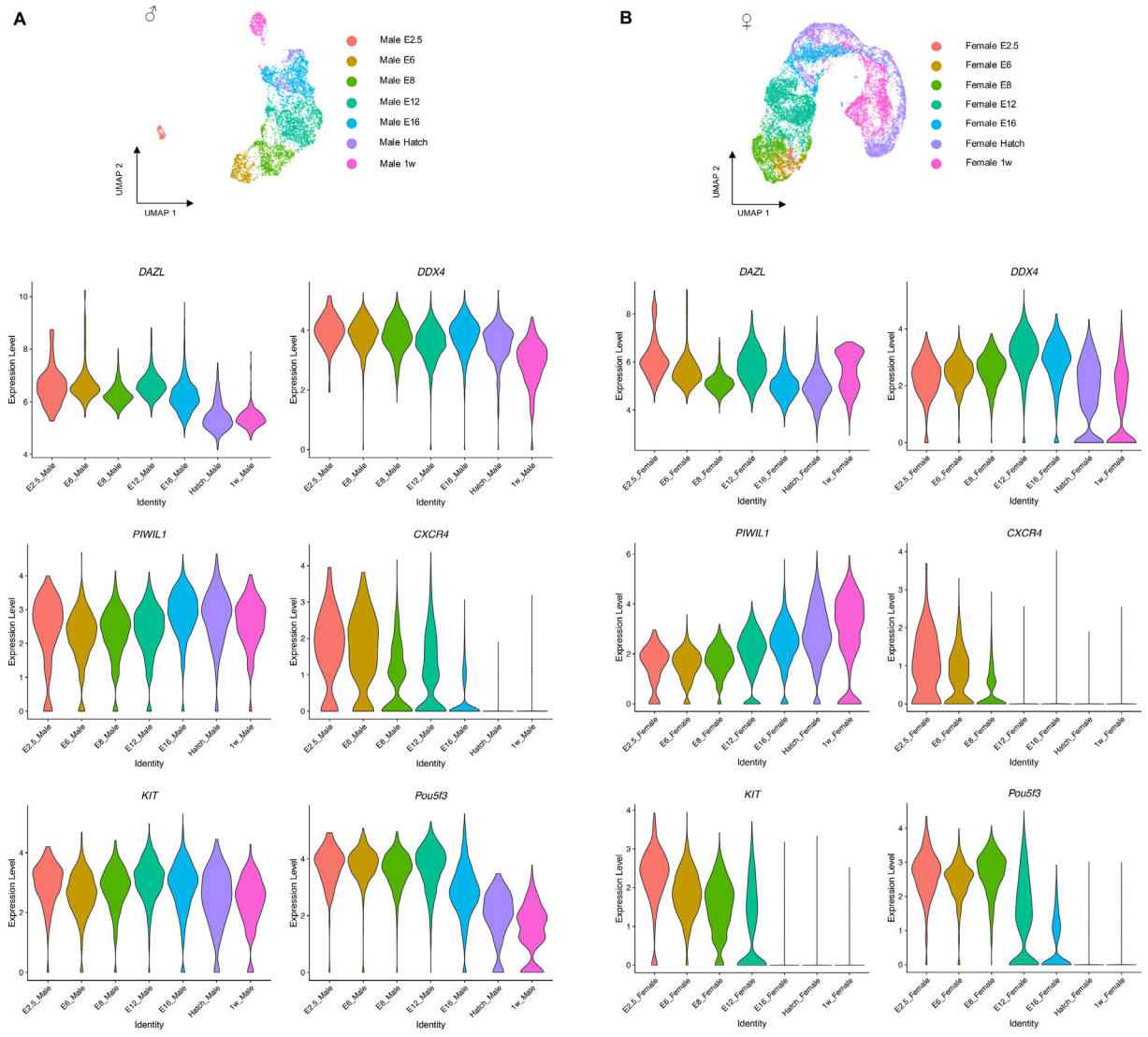

Fig. 1. Expression pattern of marker genes in male and female germ cells from *DAZL::GFP* chickens. In top, uniform manifold approximation and projection (UMAP) plot showing male and female germ cells colored by the elapsed time of development. In bottom, violin plots showing the expression of general germ cell markers (*DAZL*, *DDX4*, and *PIWIL1*), migrating germ cell markers (*CXCR4* and *KIT*), and early/mitotic germ cell marker (*Pou5f3*).

and pro-spermatogonia in males starts at about E8.0 and E13.0, respectively [9,10,37]. Also, the oogonia enter a dramatic proliferation state on E9.0 [10,11]. Therefore, we don't consider *DAZL::GFP* germ cells isolated after E8.0 as PGCs, at least in females. For these reasons, we restricted the below-mentioned scRNA-seq-based analyses from E2.5 to E8 time points in both male and female germ cells.

3.2. Transcriptome differences in male and female migrating PGCs

Based on the cells that fulfilled quality-control criteria, we prepared a single-cell transcriptome of males and females consisting *DAZL::GFP* germ cells isolated at E2.5, E6, and E8. The male scRNA-seq data comprised 126, 478, and 850 cells, respectively, at the analysis time points and are visualized by using a UMAP plot (Fig. 2A). On the other hand, the female cluster consists of 222, 675, and 1499 cells, respectively, at the analysis time points (Fig. 2B). Statistical tests were performed to identify DEGs between the male and female migrating PGCs isolated at E2.5, E6, and E8: i.e., male versus female at E2.5; male versus female at E6; and male versus female at E8. Our analysis identified a higher number of significantly upregulated genes ($P < 0.05$ and logFC > 0.5) in male PGCs at all the analysis time points (Fig. 2C, Table S1). DEGs identified between the male and female PGCs at E2.5, E6, and E8 were subjected to GOBP and KEGG pathway terms analysis to define significant sex-specific biological processes. In the results, both male- and female-specifically upregulated genes were not enriched in any sex determination related GOBP or KEGG pathway term (Table S2). Besides, male-specifically upregulated genes were enriched in the GOBP terms associated with the mitotic cell cycle (*CENPH*, *CENPK*, *RMI1*, *SMC5*, and *KIF2A*) and stem cell differentiation (*FAM172A*, *KIT*, *MSX1*, *SEMA4D*, and *SOX21*). The female-specifically upregulated genes were enriched in the GOBP terms associated with cellular metabolism (*ATP6*, *COX3*, *HNRNPKL*, *HMGB1*, *PCNA*, *TFRC*, *ENO1*, *GAPDH*, *PGAM1*, *CKB*, *NME2*, and *PPP1CB*), meiotic cell cycle (*INCENP*, *LFNG*, *RAD51*, and *RPA1*) and germ cell differentiation (*DAZL*, *LAMB1*, *LY6E*, *MAEA*, *PRTG*, and *SFRP2*) (Fig. 2D-E, Table S2). To further define significant sex-specific genes, we examined the top 25 genes that upregulated at E2.5, E6, and E8 in males or females. This analysis identified *XPA*, *GNG10*, *RPL17*, *RPS23*, and *NDUFS4* as male-specifically upregulated genes at all time points. Moreover, they are all Z sex chromosome-

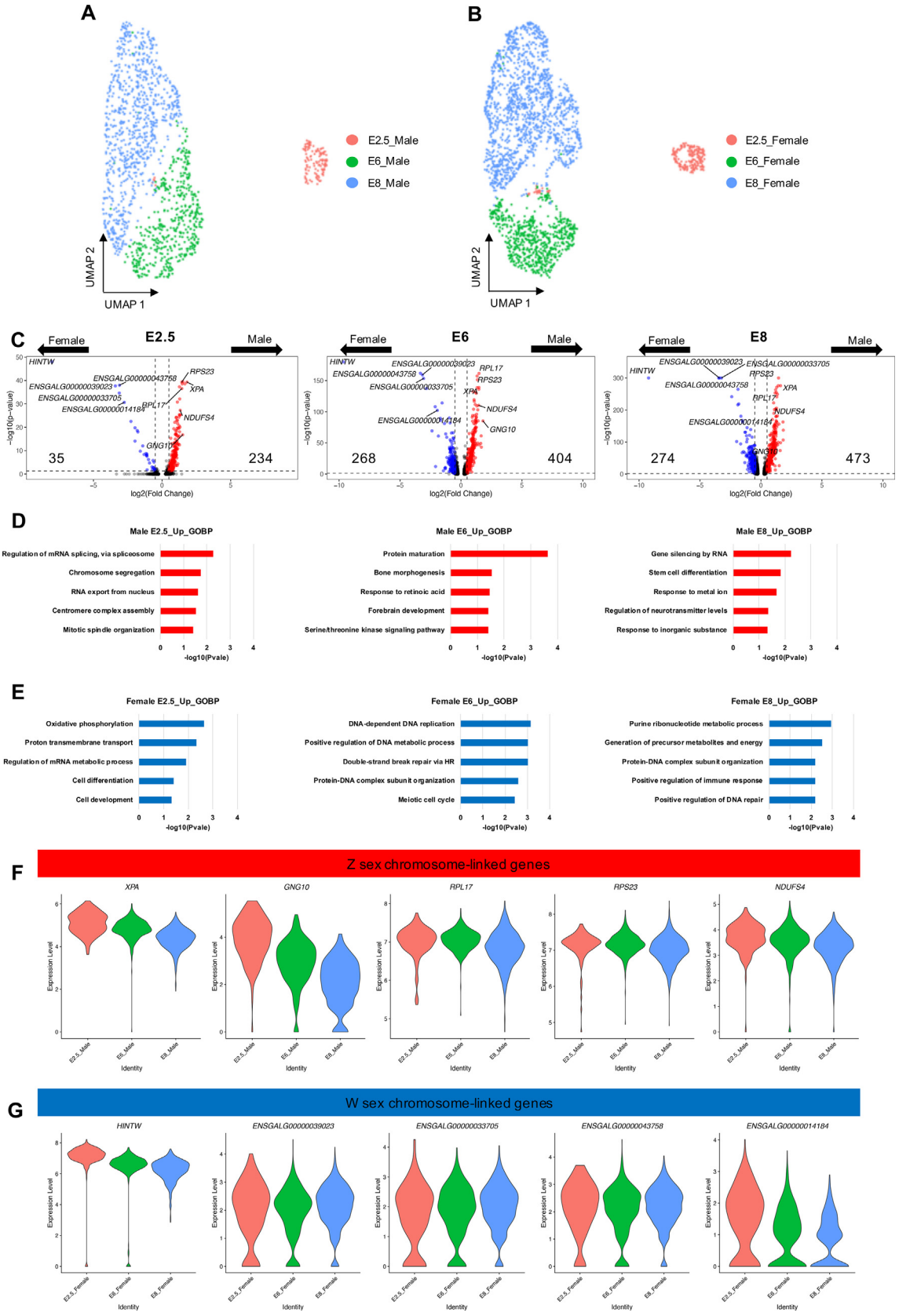

Fig. 2. Analysis of transcriptome differences in male and female chicken PGCs during their active migration time points at E2.5, E6, and E8. (A, B) Uniform manifold approximation and projection (UMAP) plots showing male (A) and female (B) cells colored by the elapsed time of development. (C) Volcano plots illustrating the differentially expressed genes (DEGs) between male and female PGCs at E2.5, E6, and E8. Red dots indicate genes significantly upregulated in male PGCs; blue dots, in female PGCs. (D, E) Representative GOBP terms of significant genes upregulated male-specifically (D) or female-specifically (E) at E2.5, E6, and E8. (F, G) Violin plots showing the top genes upregulated male-specifically (F) or female-specifically (G) at all the analysis time points. (For interpretation of the references to colour in this figure legend, the reader is referred to the web version of this article.)

linked genes (Fig. 2C and 2F). On the other hand, W sex chromosome-linked genes, including *HINTW*, *ENSGALG00000039023* (*NIPBL*), *ENSGALG00000033705* (*TERAL2*), *ENSGALG00000043758* (*ATP5F1AW*), and *ENSGALG00000014184* (*SMAD2W*) were identified as female-specifically upregulated genes at all time points (Fig. 2C and 2G). These results indicate that there are (already) differences at the transcriptome level between the male and female PGCs, although they are not entered the sex-specific pathways.

3.3. Identification of the cell cycle and transcriptionally distinct clusters in migrating PGCs

The cell cycle of each migrating PGCs from male and female chickens was inferred based on the expression of homologous genes of mouse S phase and G2/M phase, and cells that do not express S phase or G2/M phase gene sets were auto-marked as G1 phase cells. Results of these genes expression reveal that the G1, G2/M, and S phase PGCs were distributed with different percentages at each time point; however, the G2/M cells were increased among the gonadal PGCs compared to the blood PGCs in both males (Fig. 3A) and females (Fig. 3B). The G2/M genes enriched in male PGCs were *G2E3* (at E2.5 and E6), *HN1*, *CDK1*, *RANGAP1* (at E6), *CKAP5*, *TTK*, and *TOP2A* (at E8) (Fig. 3C, Table S3). Similarly, the G2/M genes enriched in female PGCs were *G2E3*, *HN1* (at E2.5 and E6), *ANP32E*, *ECT2*, *CTCF*, *LBR* (at E6), *CKS1B*, *NUF2*, *TTK*, *CKAP5*, and *DLGAP5* (at E8) (Fig. 3D, Table S3).

In the trajectory analysis using Monocle3, we found that both male (Fig. 4A) and female (Fig. 4B) germ cells linearly transitioned from E2.5 to E8. To identify transcriptionally distinct clusters in migrating PGCs from male and female chickens, unsupervised graph-based clustering was first performed with the E2.5, E6, and E8 cells. We identified 8 clusters for male PGCs: 1 cluster for E2.5 cells; 3 clusters for E6 cells; and 4 clusters for E8 cells (Fig. 4A). We identified 12 clusters for female PGCs: 1 cluster for E2.5 cells; 4 clusters for E6 cells; and 7 clusters for E8 cells (Fig. 4B). We have calculated the sufficient number of cells for scRNA-seq using single-cell one-sided probability interactive tool (SCOPIT) with default parameters [38]. According to the calculation of SCOPIT, 1312 and 1818 cells are needed to detect 8 clusters in male PGCs and 12 clusters in female PGCs, respectively. Since we analyzed 1454 male PGCs and 2396 female PGCs in this study, the cell number is enough to be analyzed through scRNA-seq. Pearson correlation between 8 male PGC clusters (Fig. 4C) and between 12 female PGC clusters (Fig. 4D) was calculated using the average expression of 750 highly variable genes (HVGs). As a result, several significant DEGs were identified in each PGCs cluster of males and females. Particularly, *ENSGALG00000048334* (lncRNA; cluster 0), *KPNA2* (cluster 1), *HES5* (clusters 2 and 3), *ENSGALG00000035994* (*ACAD6L*; cluster 4), *HBBR* (cluster 5), *RRM2* (cluster 6), and *DAZL* (cluster 7) were identified as the top genes enriched in male clusters (Table S4). The top genes enriched in female clusters were *HES5* (cluster 0), *SAT1* (cluster 1), *TPPP* (cluster 2), *KPNA2* (cluster 3), *MYLK* (cluster 4), *SMC1B* (cluster 5), *MOV10L1* (cluster 6), *AS3MT* (cluster 7), *ENSGALG00000011747* (cluster 8), *RRM2* (cluster 9), *ARHGAP11B* (cluster 10), and *HSPB9* (cluster 11) (Table S5). Furthermore, cluster 7 PGCs in males and cluster 11 PGCs in females (mostly E6 PGCs in both sex) consist of very few upregulated genes; however, nearly 150 genes were downregulated when compared to other clusters of the same sex. We noted that the *DAZL* was commonly upregulated, whereas *AMACR*, *DIEXF*, *PTGES3L*, *RBMX2*, *ENSGALG00000012766 (SYCP3)*, *ENSGALG00000013505 (SYNE1)*, and *ENSGALG00000050374* were commonly downregulated, in male cluster 7 and female cluster 11 (Fig. 4E-F, Table S4 and Table S5). Together, these data indicate that the migrating PGCs swiftly enter into the G2/M phase of the cell cycle and display heterogeneity in the gonadal environment.

3.4. Expression patterns of de novo DNA methylation, histone modification, and piRNA biogenesis genes in migrating PGCs

To investigate the scRNA-seq-based epigenetic reprogramming in migrating PGCs, we first retrieved the complete list of chicken genes associated with the AmiGO terms, such as DNA demethylation / DNA methylation and histone demethylation / histone methylation. Through mirror heatmaps, the average expression of screened genes was examined in male and female PGCs at E2.5, E6, and E8 time points. In the results, the DNA demethylation genes such as *TDG*, *GATA3*, *TOX*, *USP7*, and *TET2* were detected lower (than DNA methylation genes) in male and female PGCs at the analysis time points. Besides, the *de novo* DNA methylation, as well as maintenance of DNA methylation genes such as *MAEL*, *DNMT3A*, *BMI1*, *BEND3*, *PRMT7* (at E2.5), *HELLS*, *DNMT3B*, *PPM1D* (at E6), *ASZ1*, *KMT2E*, *DNMT1*, and *TDRD5* (at E8), were enriched in a time-dependent manner in male and female PGCs (Fig. 5A). There are also male/female differences among the expression patterns of the DNA demethylation and DNA methylation genes. For instance, the DNA methylation genes such as *BMI1*, *MPHOSPH8*, *PRDM14* (at E2.5), *DNMT3B* (at E6), *KDM1B*, *TDRKH*, *SPI1*, *N6AMT1*, *METTL4*, and *UHRF2* (at E8), were markedly higher in a time-dependent manner in male PGCs. Whereas the DNA methylation genes *PIK3CA*, *MAEL* (at E2.5), *HELLS*, *EZH2*, *PPM1D* (at E6), *MIS18A*, *DNMT1*, *TDRD5*, *KMT2E*, *ATF7IP*, *FKBP6*, and *TDRD1* (at E8), were markedly higher in a time-dependent manner in female PGCs (Fig. 5A).

In the case of histone modification programs, histone H3-R2 / H4-*R*3 / H3-K36 demethylation genes such as *JMJD6* and *KDM8* were expressed higher at E2.5 but decreased over time in male and female PGCs. The histone H3-K9 / H3-K4 / H3-K27 / H4-K20 / H3-R17 methylation genes such as *SETDB1*, *KMT2C*, *PWP1* (at E2.5), *ARID4B*, *NR1H4, MTF2* (at E6), *SUV39H2*, and *SMYD1* (at E8) were enriched in a time-dependent manner in male and female PGCs (Fig. 5B). When we considered male/female differences, for instance, the histone methylation genes such as *RTF1*, *SIRT7*, *PRDM5*, *KMT2D*, *EED*, *PRDM6*, *PRDM14* (at E2.5), *NR1H4*, *MTF2*, *ASH1L*, *ARID4B* (at E6), *RNF20*, *DOT1L*, *BCOR*, *MLLT6*, *SMYD1*, *SETDB2*, and *PAXIP1* (at E8), were markedly higher in a time-dependent manner in male PGCs. Whereas the histone methylation genes *MECOM*, *SMYD5*, *SETD1A*, *RBBP5*, *CREBBP*, *PWP1*, *KMT5C*, *SETD2* (at E2.5), *MYB*, *GFI1*, *RIF1*, *CTR9* (at E6), *WDR61*, *MTHFR*, *KPNA7*, *DNMT1*, *SETD3*, *NTMT1*, *KMT2E*, *CTNNB1*, *EHMT1*, *PRDM12*, and *PAF1* (at E8), were markedly higher in a time-dependent manner in female PGCs (Fig. 5B).

PIWI-interacting RNAs (piRNAs) are a class of small non-coding RNAs involved in the post-transcriptional regulation of genes; however, piRNAs are longer than the endogenous small-interfering RNAs (siRNAs) and micro RNAs (miRNAs). Among the small non-coding RNAs, piRNAs are germ cell-specific and primarily control transposon activity for safeguarding the germ cells genome from possible damage associated with excessive transposition [39,40]. Several pieces of evidence support a role for piRNAs, and genes involved in piRNA biogenesis (such as *PIWIs*), in PGCs specification and migration [41–43]. PIWI-piRNAs complexes guide *de novo* DNA methylation in germ cells through recognizing nascent transposable element (TE) transcripts in the nucleus and recruiting chromatin modifiers to TE genomic loci. Subsequent changes in histone marks induce the activity of the *de novo* DNA methyltransferases [44]. However, a comprehensive understanding of the expression patterns of piRNA biogenesis factor genes is not clear in the chicken PGCs. Therefore, we separately investigated the expression patterns of a set of piRNA biogenesis factor genes (ho-

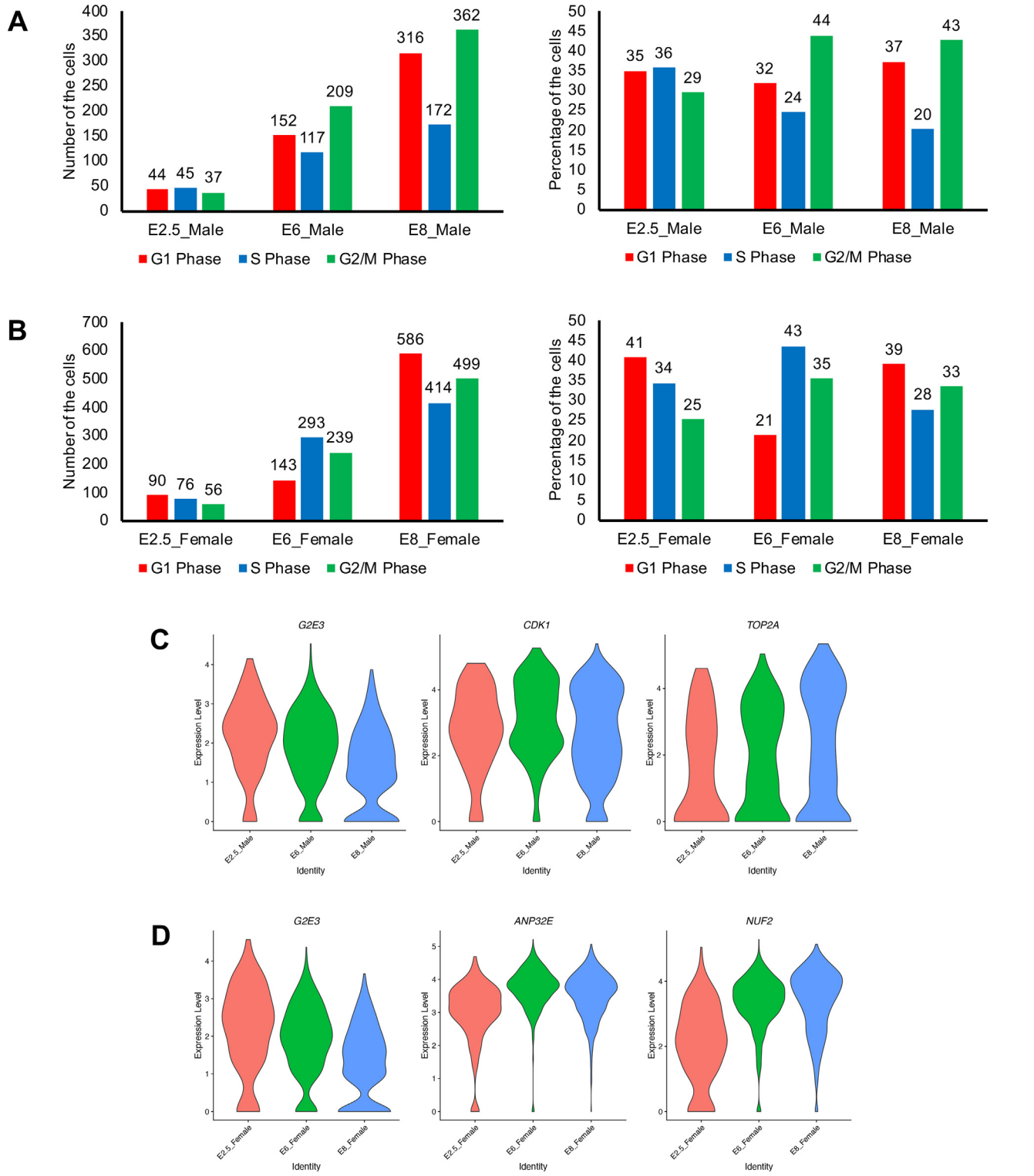

Fig. 3. Cell cycle status of male and female chicken PGCs during their active migration time points at E2.5, E6, and E8. (A, B) Number and percentage of the G1 phase, S phase, and G2/M phase PGCs identified during their active migration time points at E2.5, E6, and E8 in male (A) and female (B). (C, D) Violin plots showing the representative G2/M genes enriched in male (C) and female (D) PGCs during the elapsed time of development.

mologous mouse genes) [45] in male and female chicken PGCs at E2.5, E6, and E8 time points through a mirror heatmap. The results notably indicated that *PIWIL1*, *GPAT2*, *DDX4* (at E2.5), *HSP90AA1* (at E6), *MYBL1*, *TDRKH*, and *TDRD7* (at E8), were markedly higher in a time-dependent manner in male PGCs. *MAEL* (at E2.5), *TDRD1*, *TDRD5*, *FKBP6*, and *HENMT1* (at E8), were markedly higher in a time-dependent manner in female PGCs. Moreover, several genes, such as *GTSF1*, *ASZ1*, *MOV10L1*, and *TDRD9*, were enriched simultaneously (at E8) in both male and female PGCs (Fig. S1). These data indicate that the migrating PGCs at E2.5 establish (*de novo*) DNA

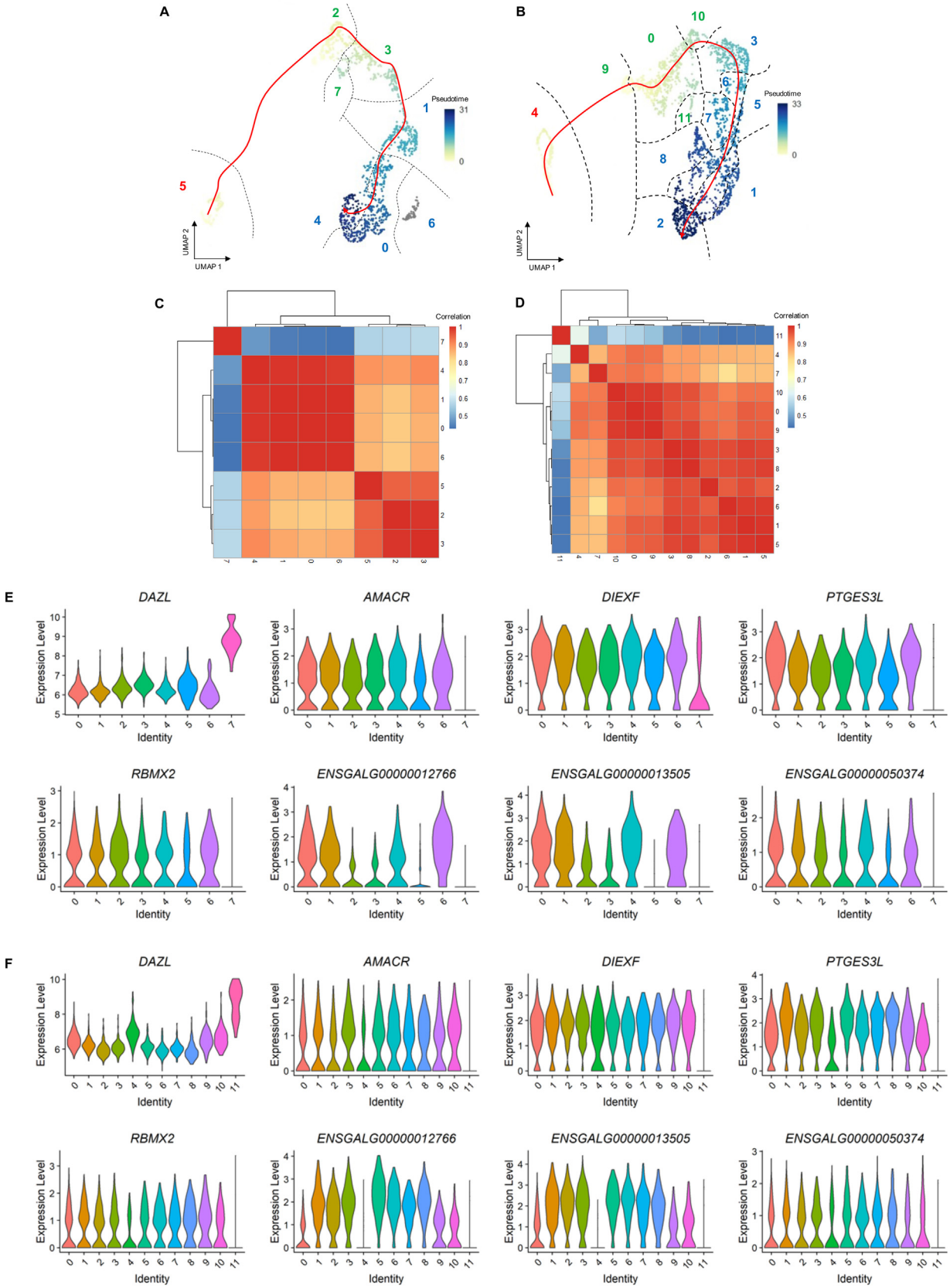

Fig. 4. Developmental trajectories and transcriptionally distinct clusters of male and female chicken PGCs during their active migration time points at E2.5, E6, and E8. (A, B) Uniform manifold approximation and projection (UMAP) plots showing male (A) and female (B) cells colored by pseudotime calculated by Monocle3. The red line on the UMAP plot indicates the linear trajectories of the male and female germ cells. The numbers on the UMAP plot indicate the distinct clusters calculated by graph-based unbiased clustering. Also, the numbers are colored by the elapsed time of development: red, E2.5; green, E6; and blue, E8. (C, D) Pearson correlation between male PGC clusters (C) and female PGC clusters (D) using average expression of 750 highly variable genes (HVGs). (E, F) Violin plots illustrating the normalized expression levels of commonly upregulated and downregulated genes in cluster 7 PGCs in males (E) and cluster 11 PGCs in females (F). (For interpretation of the references to colour in this figure legend, the reader is referred to the web version of this article.)

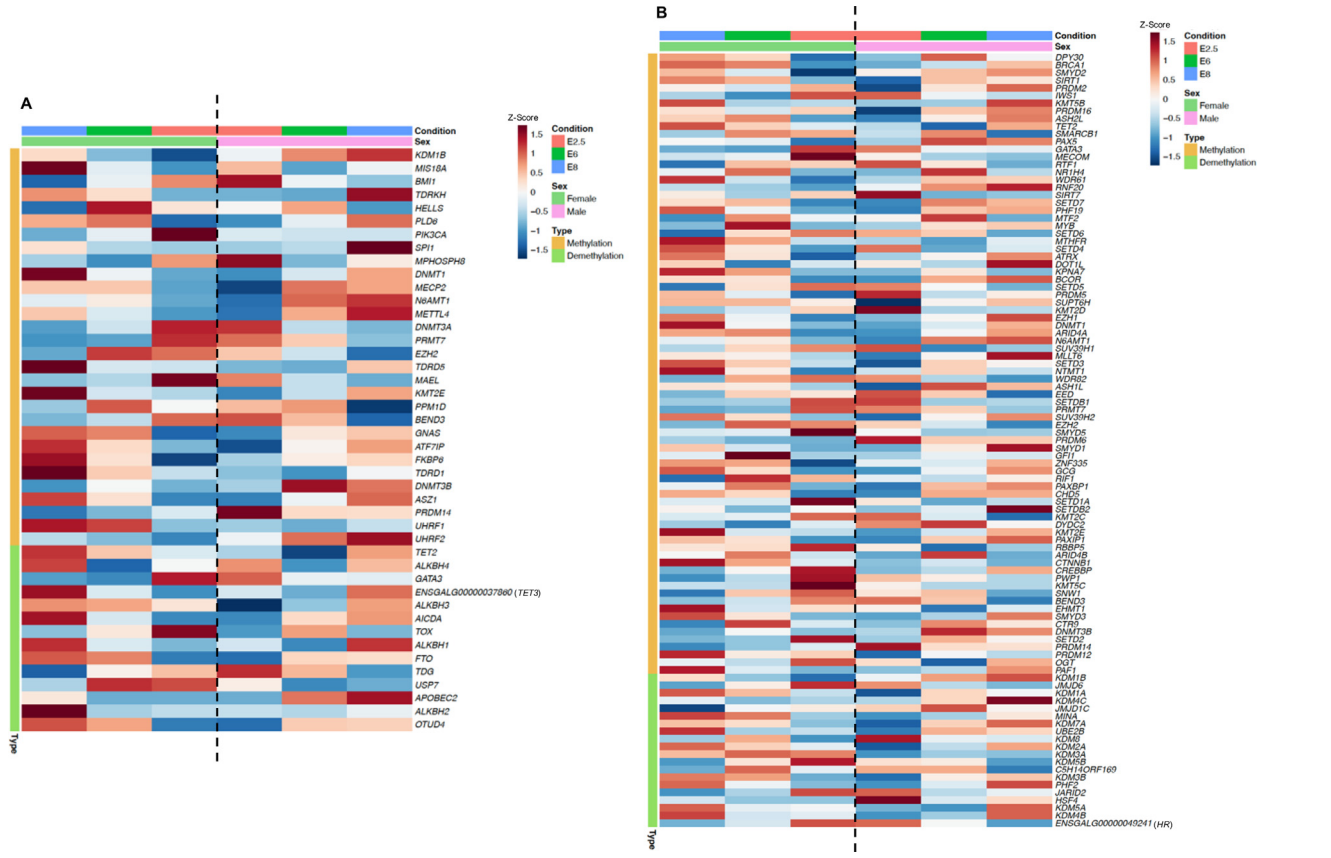

Fig. 5. Expression patterns of a set of epigenetic reprogramming genes in the chicken PGCs during their active migration time points at E2.5, E6, and E8. (A) Mirror heatmap showing the average expression patterns of genes associated with the DNA demethylation / methylation. (B) Mirror heatmap showing the average expression patterns of genes associated with the histone demethylation / methylation. In the mirror heatmaps, chicken PGCs were ordered along the time points and sex: E2.5 cells of the male and female are at the center; E6 and E8 cells of the male are at the right; E6 and E8 cells of the female are at the left.

methylation; however, they undergo histone demethylation and methylation programs. And piRNA biogenesis factors could support the establishment of *de novo* DNA methylation in migrating PGCs.

3.5. The differentially expressed genes and TFs between blood PGCs and gonadal PGCs

First, in this section, statistical tests were performed to identify DEGs between the same-sex PGCs isolated from blood circulation at E2.5, and from gonads at E6 and E8: i.e., E2.5 versus E6; E2.5 versus E8; and E6 versus E8. Results in males reveals 360 upregulated genes and 370 downregulated genes in E2.5 cells compared to E6 cells; 1008 upregulated genes and 595 downregulated genes in E2.5 cells compared to E8 cells (P < 0.05 and logFC > 0.5 or <−0.5) (Fig. 6A, Table S6). A similar analysis in females reveals 296 upregulated genes and 154 downregulated genes in E2.5 cells compared to E6 cells; 688 upregulated genes and 339 downregulated genes in E2.5 cells compared to E8 cells (Fig. 6B, Table S7). These data further indicate larger differences in gene expression between the blood PGCs and gonadal PGCs in males than in females.

We next examined the common and sex-specific DEGs in blood PGCs compared to gonadal PGCs. As a result, 189 upregulated genes and 98 downregulated genes were commonly identified in E2.5 cells compared to E6 cells; 171 upregulated genes and 272 downregulated genes were male-specifically identified in E2.5 cells compared to E6 cells; 107 upregulated genes and 56 downregulated genes were female-specifically identified in E2.5 cells compared to E6 cells (Fig. 6C, Table S8, Fig. S2). Similarly, 548 upregulated genes and 246 downregulated genes were commonly identified in E2.5 cells compared to E8 cells; 460 upregulated genes and 349 downregulated genes were male-specifically identified in E2.5 cells compared to E8 cells; 140 upregulated genes and 93 downregulated genes were female-specifically identified in E2.5 cells compared to E8 cells (Fig. 6C, Table S8, Fig. S3). Also, several DEGs were commonly, male-specifically, or female-specifically identified in E6 cells compared to E8 cells (Fig. 6C, Table S8, Fig. S4). To further define the functions of these common and sex-specific DEGs in blood PGCs, they were subjected to GOBP terms and KEGG pathways analysis. Collectively, a significant proportion of male-specifically upregulated genes in blood PGCs was found to involve in various biological processes, mainly related to positive regulation of cell cycle, positive regulation of cell death, and p53 signaling pathway, which involved in the selection of only mature functional cells during germ cells migration (Table S9). The female-specifically upregulated genes in blood PGCs were also found to involve in various biological processes; however, they related to response to retinoic acid, female gonad development, BMP signaling pathway, JAK-STAT signaling pathway, MAPK signaling pathway, FoxO signaling pathway, Notch signaling pathway, and NOD-like receptor signaling pathway, which could be necessary for the migration of female PGCs (Table S9).

All the DEGs above were mapped with the *Gallus gallus* TF list of AnimalTFDB3.0 to identify the TFs among the gene list. Results of this analysis reveal a number of the common and sex-specific differentially expressed TFs in blood PGCs compared to gonadal PGCs (Fig. 7A, Table S10). *TCF7L2*, *HHEX*, *SMAD2Z*, *BHLHE22*, *TFAP2A*, *CARHSP1*, *SALL4*, *NOTO*, *ETV1*, *SETDB1*, *SALL1*, *GLI3*, *EOMES*, and *ETV5*, were significantly upregulated in E2.5 cells compared to both E6 and E8 cells in male and female. Besides, *HES5*,

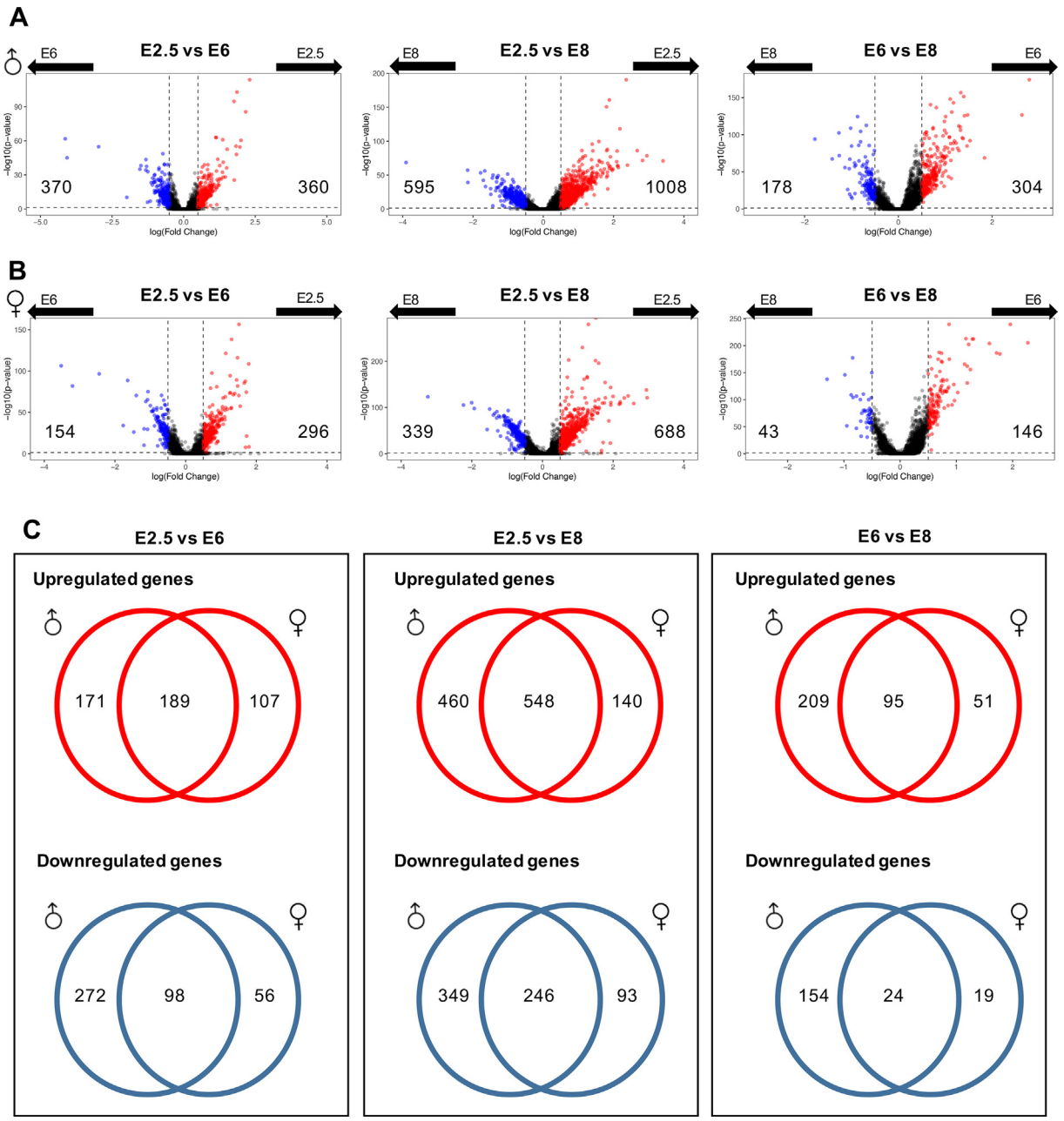

Fig. 6. Differentially expressed genes (DEGs) between the blood PGCs and gonadal PGCs in chicken. (A) Volcano plots illustrating the DEGs between male PGCs: E2.5 vs E6; E2.5 vs E8; and E6 vs E8. (B) Volcano plots illustrating the DEGs between female PGCs: E2.5 vs E6; E2.5 vs E8; and E6 vs E8. In A and B, red and blue dots indicate genes significantly upregulated in the specified cells of the respective sex. (C) Venn diagram showing the significant DEGs identified commonly, male-specifically, or female-specifically between the PGCs isolated at E2.5, E6, and E8. (For interpretation of the references to colour in this figure legend, the reader is referred to the web version of this article.)

ENSGALG00000035951, *MYF6*, *DMRT1*, *SP5*, and *HMGB2*, were significantly downregulated in E2.5 cells compared to both E6 and E8 cells in males and females (Fig. 7B-C, Table S10). Results of this analysis further reveal that, similar to the DEGs analysis, large numbers of TFs were identified as upregulated and downregulated in male blood PGCs than in female blood PGCs (Fig. 7A, Table S10). Together, these data provide insight into DEGs (including TFs) and associated functions in blood PGCs and gonadal PGCs.

4. Discussion and conclusion

After specification by epigenesis mode or inherited mode, the newly formed PGCs stay in the non-motile phase for a while. Subsequently, the germ cells polarize and migrate passively by the morphogenetic movement of the embryo or migrate actively through signaling molecules towards the genital ridge. In chickens, the PGCs are non-motile from EGK stage-III to stage-X. At about HH stage-2, PGCs polarize and move passively toward the anterior region by the morphogenetic movement of the embryo [8,23]. Further migration of PGCs towards the genital ridge via the germinal crescent region and blood vessels is achieved actively through the interaction of signaling molecules, such as CXCR4 and SDF1 [6,23]. However, a comprehensive understanding of the transcriptional programming of PGCs during their active migration is still inadequate, mainly due to the technologies lacking for the isolation of pure PGCs. The scRNA-seq technology allows transcriptional

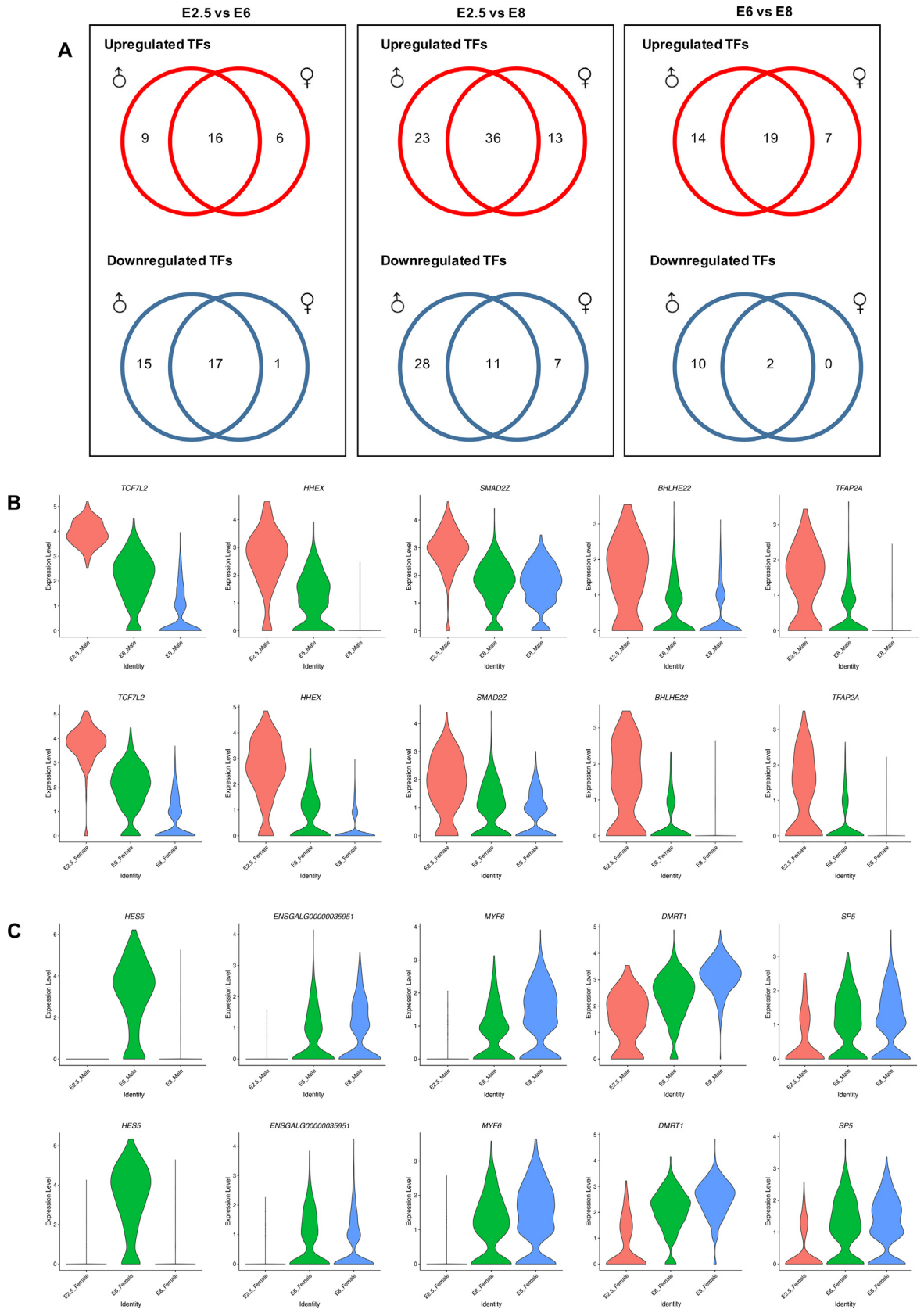

Fig. 7. Differentially expressed transcription factors (TFs) between the blood PGCs and gonadal PGCs in chicken. (A) Venn diagram showing the significant TFs identified commonly, male-specifically, or female-specifically between the PGCs isolated at E2.5, E6, and E8. (B) Violin plots showing representative TFs commonly upregulated in E2.5 PGCs compared to both E6 and E8 PGCs in males and females. (C) Violin plots showing representative TFs commonly downregulated in E2.5 PGCs compared to both E6 and E8 PGCs in males and females. (For interpretation of the references to colour in this figure legend, the reader is referred to the web version of this article.)

profiling at the single-cell level from tens of thousands of single cells and helps to uncover new and unexpected biological discoveries [46]. In this study, we analyzed the same scRNA-seq dataset of PGCs from *DAZL::GFP* chickens at E2.5, E6, and E8, reported in our earlier study [24], to uncover the transcriptional programming of PGCs during their active migration. Due to restricted analysis within a small-time frame, these results are stand-alone from our earlier study.

After the PGCs entered the gonad, they will associate with the gonadal somatic cells and start to perform their functions as male or female germ cells. Although the PGCs have their own sex chromosome pattern, their sexual fates are determined by the sexual identity of the embryonic gonad, in which the PGCs settle down [13,47]. Therefore, a sign of sex-specific differences during PGC migration is largely deficient in any organism. In mice, PGCs arise at E6.25, start migration at E8, and enter the genital ridge at E10.5 [19]. A recent scRNA-seq study in mice revealed that the transcriptome of male and female PGCs overlap globally at early stages (E9.0, E10.5, and E11.5). In contrast, the cells sharply show sex-specific pathways after E11.5 by upregulating downstream Nodal/Activin genes in male and BMP genes in female [48]. In our study, the transcriptome of male and female PGCs show a considerable level of differences right from E2.5. In the GOBP and KEGG pathway analysis, several terms were differentially enriched in male PGCs or female PGCs, although the sex determination term was not enriched. Also, we identified several Z-linked (*XPA*, *GNG10*, *RPL17*, *RPS23*, and *NDUFS4*) or W-linked (*HINTW*, *NIPBL*, *TERAL2*, *ATP5F1AW*, and *SMAD2W*) genes that continuously upregulated male-specifically or female-specifically, indicating a sign for sex-specific differences during PGC migration. Among all these mentioned genes, only two were known to be involved in sex determination. *HINTW* was reported as a ubiquitously expressed gene; however, a strong female-sex determining gene in chicken [49,50]. The W/Z length polymorphisms of *NIPBL* were successfully used for the sexing of bird species, such as Psittaciformes (parrots), in which sexing is difficult because they show no sexual dimorphism [51].

In our investigation, the proportion of G2/M cells was detected in an increasing trend from E2.5 to E8, along with the expression of migrating germ cell marker *CXCR4* [6] and early/mitotic germ cell marker *Pou5f3* [52], indicating that the migrating PGCs are mitotically active. scRNA-seq is an innovative technique to identify the transcriptionally distinct clusters and heterogeneity of PGCs. In a recent study, five transcriptionally distinct clusters, characterized by non-proliferative (G1) cluster, mitotically active (G2/M or S) cluster, higher mitochondrial genes and lower ribosomal genes expressing cluster, higher ribosomal proteins and lower *STRA8* expressing cluster, and *POU5F3* expressing cluster, were identified in the gonadal PGCs and germ cells (E4.5 to E10.5) of chickens using scRNA-seq [53]. In another avian species, the zebra finch (*Taeniopygia guttata*), three transcriptionally distinct clusters, characterized by low pluripotency/germness subtype, high germness subtype, and high pluripotency subtype, were identified in the gonadal PGCs (E5.5–6 / HH stage-28) using scRNA-seq [54]. Among the non-avian species, seven transcriptionally distinct clusters, such as early PGCs cluster, late PGCs (oogonia) cluster, pre-leptotene cluster, leptotene cluster, zygotene cluster, early pachytene cluster, and late pachytene cluster, were identified particularly in the female gonadal germ cells (E12.5 to E16.5) of mice using scRNA-seq [55]. In our study, 8 clusters for male PGCs and 12 clusters for female PGCs were identified, and mostly E6 and E8 cells were sub-clustered, indicating their heterogeneity in the gonadal environment. When we analyzed the genes enriched in each PGCs cluster, cluster 7 in males and cluster 11 in females were identified as more distinct clusters. These clusters contain mostly E6 cells, very few upregulated genes, and nearly 150 downregulated genes. Notably, these clusters were characterized by the common upregulation of *DAZL*. In mice, deficiency of *DAZL* does not affect the specification and migration of PGCs, but *DAZL* is required for the commitment of PGCs to the sex-specific pathways of oogenesis and spermatogenesis in sexually differentiated gonads [47]. In chickens, *DAZL* can be critical for the specification and migration of PGCs and later germ cell development because of its continuous expression from the inherited germ plasm of oocytes to all subsequent stages of germ cell development [7,56]. Moreover, the DAZL interacts with thousands of genes to enhance the translation of genes that are critical for the normal functioning of germ cells at various stages and for repressing the translation of genes that affect the survivability of germ cells [57–59]. Therefore, we believe that the *DAZL* upregulation in male cluster 7 and female cluster 11 could enhance the translation of its interacting genes critical for germ cell development and downregulated here. For instance, *SYCP3* (which encodes synaptonemal complex protein) is crucial for the male and female germ cells to enter the meiosis [10]. *MOV10L1*, a testis-specific RNA helicase, is a master piRNA biogenesis regulator that protects the genome integrity of the germline [60]. The translation of the cohesin formation gene, *SMC1B*, is stimulated in the human fetal ovary by the presence of DAZL but not by a mutant DAZL [61].

Epigenetic reprogramming is a hallmark property of migrating PGCs. In mammals, the genome-wide DNA demethylation occurs in migrating PGCs, and the re-establishment of DNA methylation and its maintenance occurs in germ cells after colonization; however, in embryonic gonads in males and postnatal gonads in females [1,62]. Also, the DNA methylation program is closely linked with histone modification and the chromatin remodeling [63]. In mammals, it was reported that the migrating PGCs undergo several histone modifications, including the loss of H3K9me2 and gaining of H3K27me3, H2A/H4R3me2 [1,64]. Moreover, most epigenetic reprogramming mechanisms are achieved by a time-dependent expression or repression of marker genes (such as *PRDMs*, *DNMTs*, *TETs*, *HDACs*, and *JMJDs*) in germ cells [1,63–65]. To investigate scRNA-seq-based epigenetic reprogramming and to identify novel genes in chicken PGCs, we examined the expression patterns of a set of genes associated with the DNA demethylation / methylation and histone demethylation / methylation. Although there are differences between the gene expression in male and female PGCs, several *de novo* methylation as well as maintenance of methylation-related genes such as *MAEL* and *BMI1* (at E2.5), *HELLS* and *PPM1D* (at E6), and *ASZ1* and *KMT2E* (at E8) were enriched in both male and female PGCs together with the previously known DNA methylation related genes *DNMT3A*, *DNMT3B*, and *DNMT1* [17]. Additionally, the higher expression of *HELLS* in chicken PGCs was reported recently [66]. Furthermore, the expression of *DNMT3A* was detected equally higher in both male and female PGCs at E2.5 in this study, indicating the establishment of *de novo* DNA methylation in both male and female PGCs at the same time. Although the expression of *PIWIL1* was slightly different in males and females, it could support the establishment of *de novo* DNA methylation in migrating PGCs. In contrast to *DNMT3A*, the expression of *DNMT1*, which involves the maintenance of methylation, was markedly higher in female PGCs at E8 than in male PGCs, indicating that the gene could prepare female PGCs for early entry into oogenesis. To our knowledge, the histone demethylation / methylation genes enriched in a time-dependent manner in this study are also novel in chicken PGCs. They need further experimental validation in future studies.

Several studies have attempted to distinguish the phenotypic differences of blood PGCs from gonadal PGCs in chickens [67,68]; however, differences in transcriptional programming are not well-known. In this study, we found a large number of DEGs in blood PGCs (E2.5) compared to gonadal PGCs (E8) in both males and females, indicating that the transcriptional programs of these

cells are largely distinct. Moreover, the identified DEGs in male blood PGCs are quite higher than that of female blood PGCs, indicating the superior transcriptional programs in male PGCs, even though both cells are migrating towards the genital ridge. Furthermore, the enriched biological processes and pathways of DEGs can be important for the migration of chicken PGCs, as reported partly in previous studies. Adherens junction, Wnt-signaling, TGFβ-signaling, and hedgehog signaling are particularly important for the PGCs migration and proliferation [13,20–22,69]. The TFs critically required for the migrating PGCs, circulating/blood PGCs in the case of chicken, is less known in many species. Sun et al. reported that the mouse embryos carrying homozygous null mutations in *Msx1* and *Msx2*, both are homeobox-containing TFs, show defects in PGCs migration and a reduced number of PGCs [70]. To uncover the above deficiency in chickens, we identified the differentially expressed TFs in blood PGCs (E2.5) compared to gonadal PGCs (E6 and E8). In correlation with DEGs analysis, we found a higher number of differentially expressed TFs in male blood PGCs compared to female blood PGCs. In conclusion, we analyzed the transcriptional programming of chicken PGCs during their active migration phase (from E2.5 to E8) with scRNA-seq. Our results highlight the molecular characteristics (including the sex-specific differences, distinct clusters, epigenetic reprogramming, and DEGs/TFs) of migrating PGCs with particular emphasis on blood PGCs compared to gonadal PGCs.

Declaration of Competing Interest

The authors declare that they have no known competing financial interests or personal relationships that could have appeared to influence the work reported in this paper.

Acknowledgments

This work was supported by the (NRF) grant funded by the Korea government (MSIP) (No. NRF-2015R1A3A2033826). We are grateful to Dr. Jong Kyoung Kim, Ph.D. (Department of Life Sciences, Pohang University of Science and Technology [POSTECH], Pohang, Korea) for valuable suggestions.

CRediT authorship contribution statement

Deivendran Rengaraj: Conceptualization, Methodology, Software, Investigation, Visualization, Writing – original draft, Writing – review & editing. **Dong Gon Cha:** Conceptualization, Methodology, Software, Investigation, Visualization, Writing – original draft, Writing – review & editing. **Kyung Je Park:** Resources. **Kyung Youn Lee:** Resources, Writing – review & editing. **Seung Je Woo:** Resources. **Jae Yong Han:** Conceptualization, Supervision, Funding acquisition, Writing – review & editing.

Data and code availability

The single-cell RNA sequencing data have been deposited in the SRA database under the accession code PRJNA761874. The scripts and instances used for the analysis of the single-cell RNA sequencing data are uploaded in the GitHub: https://github.com/dgcha97/Chicken_GermCell_2nd.

Ethics approval

All experimental procedures and care of chickens was approved by the Institute of Laboratory Animal Resources, Seoul National University, Korea, and all methods were carried out in accordance with ARRIVE (Animal Research: Reporting of In Vivo Experiments) guidelines and approved by the Institutional Animal Care and Use Committee (IACUC, SNU-190401-1–1) of Seoul National University, Korea.

Consent to participate

Not applicable.

Consent for publication

Not applicable.

Appendix A. Supplementary data

Supplementary data to this article can be found online at https://doi.org/10.1016/j.csbj.2022.10.034.

References

[1] Tang WW, Kobayashi T, Irie N, et al. Specification and epigenetic programming of the human germ line. Nat Rev Genet 2016;17:585–600.
[2] Jamieson-Lucy A, Mullins MC. The vertebrate Balbiani body, germ plasm, and oocyte polarity. Curr Top Dev Biol 2019;135:1–34.
[3] Tsunekawa N, Naito M, Sakai Y, et al. Isolation of chicken vasa homolog gene and tracing the origin of primordial germ cells. Development 2000;127:2741–50.
[4] Eyalgiladi H, Kochav S. From cleavage to primitive streak formation: a complementary normal table and a new look at the first stages of the development of the Chick. I General morphology. Dev Biol 1976;49:321–37.
[5] Hamburger V, Hamilton HL. A series of normal stages in the development of the chick embryo. J Morphol 1951;88:49–92.
[6] Stebler J, Spieler D, Slanchev K, et al. Primordial germ cell migration in the chick and mouse embryo: the role of the chemokine SDF-1/CXCL12. Dev Biol 2004;272:351–61.
[7] Lee HC, Choi HJ, Lee HG, et al. DAZL expression explains origin and central formation of primordial germ cells in chickens. Stem Cells Dev 2016;25:68–79.
[8] Kim YM, Han JY. The early development of germ cells in chicken. Int J Dev Biol 2018;62:145–52.
[9] Nakamura Y, Yamamoto Y, Usui F, et al. Migration and proliferation of primordial germ cells in the early chicken embryo. Poult Sci 2007;86:2182–93.
[10] Zheng YH, Rengaraj D, Choi JW, et al. Expression pattern of meiosis associated SYCP family members during germline development in chickens. Reproduction 2009;138:483–92.
[11] Yang SY, Lee HJ, Lee HC, et al. The dynamic development of germ cells during chicken embryogenesis. Poult Sci 2018;97:650–7.
[12] Tarbashevich K, Raz E. The nuts and bolts of germ-cell migration. Curr Opin Cell Biol 2010;22:715–21.
[13] Richardson BE, Lehmann R. Mechanisms guiding primordial germ cell migration: strategies from different organisms. Nat Rev Mol Cell Biol 2010;11:37–49.
[14] Kuwana T, Rogulska T. Migratory mechanisms of chick primordial germ cells toward gonadal anlage. Cell Mol Biol (Noisy-le-grand) 1999;45:725–36.
[15] Urven LE, Abbott UK, Erickson CA. Distribution of extracellular matrix in the migratory pathway of avian primordial germ cells. Anat Rec 1989;224:14–21.
[16] Huss DJ, Saias S, Hamamah S, et al. Avian primordial germ cells contribute to and interact with the extracellular matrix during early migration. Front Cell Dev Biol 2019;7:35.
[17] Rengaraj D, Lee BR, Lee SI, et al. Expression patterns and miRNA regulation of DNA methyltransferases in chicken primordial germ cells. PLoS ONE 2011;6:e19524.
[18] Lavial F, Acloque H, Bertocchini F, et al. The Oct4 homologue PouV and Nanog regulate pluripotency in chicken embryonic stem cells. Development 2007;134:3549–63.
[19] Tang WW, Dietmann S, Irie N, et al. A unique gene regulatory network resets the human germline epigenome for development. Cell 2015;161:1453–67.
[20] Chawengsaksophak K, Svingen T, Ng ET, et al. Loss of Wnt5a disrupts primordial germ cell migration and male sexual development in mice. Biol Reprod 2012;86:1–12.
[21] Whyte J, Glover JD, Woodcock M, et al. FGF, insulin, and SMAD signaling cooperate for avian primordial germ cell self-renewal. Stem Cell Rep 2015;5:1171–82.
[22] Lee HC, Lim S, Han JY. Wnt/beta-catenin signaling pathway activation is required for proliferation of chicken primordial germ cells in vitro. Sci Rep 2016;6:34510.
[23] Kang KS, Lee HC, Kim HJ, et al. Spatial and temporal action of chicken primordial germ cells during initial migration. Reproduction 2015;149:179–87.
[24] Rengaraj D, Cha DG, Lee HJ, et al. Dissecting chicken germ cell dynamics by combining a germ cell tracing transgenic chicken model with single-cell RNA sequencing. Comput Struct Biotechnol J 2022;20:1654–69.

[25] Park TS, Han JY. piggyBac transposition into primordial germ cells is an efficient tool for transgenesis in chickens. Proc Natl Acad Sci USA 2012;109:9337–41.
[26] Dobin A, Davis CA, Schlesinger F, et al. STAR: ultrafast universal RNA-seq aligner. Bioinformatics 2013;29:15–21.
[27] Lun ATL, Riesenfeld S, Andrews T, et al. EmptyDrops: distinguishing cells from empty droplets in droplet-based single-cell RNA sequencing data. Genome Biol 2019;20:63.
[28] McCarthy DJ, Campbell KR, Lun AT, et al. Scater: pre-processing, quality control, normalization and visualization of single-cell RNA-seq data in R. Bioinformatics 2017;33:1179–86.
[29] Lun AT, McCarthy DJ, Marioni JC. A step-by-step workflow for low-level analysis of single-cell RNA-seq data with Bioconductor. F1000Res 2016;5:2122.
[30] Satija R, Farrell JA, Gennert D, et al. Spatial reconstruction of single-cell gene expression data. Nat Biotechnol 2015;33:495–502.
[31] Kanehisa M, Goto S. KEGG: kyoto encyclopedia of genes and genomes. Nucleic Acids Res 2000;28:27–30.
[32] Tenenbaum D. KEGGREST: Client-side REST access to KEGG. R Package Version 1.20.0 ed2018.
[33] Cao J, Spielmann M, Qiu X, et al. The single-cell transcriptional landscape of mammalian organogenesis. Nature 2019;566:496–502.
[34] Ashburner M, Ball CA, Blake JA, et al. Gene ontology: tool for the unification of biology. The Gene Ontology Consortium. Nat Genet 2000;25:25–9.
[35] Gene Ontology Consortium. The gene ontology resource: enriching a GOld mine. Nucleic Acids Res 2021;49:D325-D334.
[36] Hu H, Miao YR, Jia LH, et al. AnimalTFDB 3.0: a comprehensive resource for annotation and prediction of animal transcription factors. Nucleic Acids Res 2019;47:D33–8.
[37] Aramaki S, Sato F, Kato T, et al. Molecular cloning and expression of dead end homologue in chicken primordial germ cells. Cell Tissue Res 2007;330:45–52.
[38] Davis A, Gao R, Navin NE. SCOPIT: sample size calculations for single-cell sequencing experiments. BMC Bioinf 2019;20:566.
[39] Aravin A, Gaidatzis D, Pfeffer S, et al. A novel class of small RNAs bind to MILI protein in mouse testes. Nature 2006;442:203–7.
[40] Banisch TU, Goudarzi M, Raz E. Small RNAs in germ cell development. Curr Top Dev Biol 2012;99:79–113.
[41] Li M, Hong N, Gui J, et al. Medaka piwi is essential for primordial germ cell migration. Curr Mol Med 2012;12:1040–9.
[42] Kim TH, Yun TW, Rengaraj D, et al. Conserved functional characteristics of the PIWI family members in chicken germ cell lineage. Theriogenology 2012;78:1948–59.
[43] Rengaraj D, Lee SI, Park TS, et al. Small non-coding RNA profiling and the role of piRNA pathway genes in the protection of chicken primordial germ cells. BMC Genomics 2014;15:757.
[44] Aravin AA, Bourc'his D. Small RNA guides for de novo DNA methylation in mammalian germ cells. Gene Dev 2008;22:970–5.
[45] Sun YH, Lee B, Li XZ. The birth of piRNAs: how mammalian piRNAs are produced, originated, and evolved. Mamm Genome 2022;33:293–311.
[46] Hwang B, Lee JH, Bang D. Single-cell RNA sequencing technologies and bioinformatics pipelines. Exp Mol Med 2018;50:1–14.
[47] Gill ME, Hu YC, Lin Y, et al. Licensing of gametogenesis, dependent on RNA binding protein DAZL, as a gateway to sexual differentiation of fetal germ cells. Proc Natl Acad Sci USA 2011;108:7443–8.
[48] Mayere C, Neirijnck Y, Sararols P, et al. Single-cell transcriptomics reveal temporal dynamics of critical regulators of germ cell fate during mouse sex determination. FASEB J 2021;35:e21452.
[49] Smith CA, Roeszler KN, Sinclair AH. Genetic evidence against a role for W-linked histidine triad nucleotide binding protein (HINTW) in avian sex determination. Int J Dev Biol 2009;53:59–67.
[50] Sun C, Jin K, Zhou J, et al. Role and function of the Hintw in early sex differentiation in chicken (Gallus gallus) embryo. Anim Biotechnol 2021:1–11.
[51] Kroczak A, Woloszynska M, Wierzbicki H, et al. New bird sexing strategy developed in the order Psittaciformes involves multiple markers to avoid sex misidentification: Debunked myth of the universal DNA marker. Genes 2021;12:878.
[52] Li L, Dong J, Yan L, et al. Single-cell RNA-seq analysis maps development of human germline cells and gonadal niche interactions. Cell Stem Cell 2017;20:858–873.e4.
[53] Estermann MA, Williams S, Hirst CE, et al. Insights into gonadal sex differentiation provided by single-cell transcriptomics in the chicken embryo. Cell Rep 2020;31:107491.
[54] Jung KM, Seo M, Kim YM, et al. Single-cell RNA sequencing revealed the heterogeneity of gonadal primordial germ cells in zebra finch (Taeniopygia guttata). Front Cell Dev Biol 2021;9:791335.
[55] Zhao ZH, Ma JY, Meng TG, et al. Single-cell RNA sequencing reveals the landscape of early female germ cell development. FASEB J 2020;34:12634–45.
[56] Rengaraj D, Zheng YH, Kang KS, et al. Conserved expression pattern of chicken DAZL in primordial germ cells and germ-line cells. Theriogenology 2010;74:765–76.
[57] Chen HH, Welling M, Bloch DB, et al. DAZL limits pluripotency, differentiation, and apoptosis in developing primordial germ cells. Stem Cell Rep 2014;3:892–904.
[58] Li H, Liang Z, Yang J, et al. DAZL is a master translational regulator of murine spermatogenesis. Natl Sci Rev 2019;6:455–68.
[59] Rengaraj D, Won S, Han JW, et al. Whole-transcriptome sequencing-based analysis of DAZL and its interacting genes during germ cells specification and zygotic genome activation in chickens. Int J Mol Sci 2020;21:8170.
[60] Fu Q, Pandey RR, Leu NA, et al. Mutations in the MOV10L1 ATP hydrolysis motif cause piRNA biogenesis failure and male sterility in mice. Biol Reprod 2016;95:103.
[61] Rosario R, Smith RW, Adams IR, et al. RNA immunoprecipitation identifies novel targets of DAZL in human foetal ovary. Mol Hum Reprod 2017;23:177–86.
[62] Kobayashi H, Sakurai T, Miura F, et al. High-resolution DNA methylome analysis of primordial germ cells identifies gender-specific reprogramming in mice. Genome Res 2013;23:616–27.
[63] Li E. Chromatin modification and epigenetic reprogramming in mammalian development. Nat Rev Genet 2002;3:662–73.
[64] Seki Y, Yamaji M, Yabuta Y, et al. Cellular dynamics associated with the genome-wide epigenetic reprogramming in migrating primordial germ cells in mice. Development 2007;134:2627–38.
[65] Ambrosi C, Manzo M, Baubec T. Dynamics and context-dependent roles of DNA methylation. J Mol Biol 2017;429:1459–75.
[66] Kress C, Montillet G, Jean C, et al. Chicken embryonic stem cells and primordial germ cells display different heterochromatic histone marks than their mammalian counterparts. Epigenetics Chromatin 2016;9:5.
[67] Naeemipour M, Dehghani H, Bassami M, et al. Expression dynamics of pluripotency genes in chicken primordial germ cells before and after colonization of the genital ridges. Mol Reprod Dev 2013;80:849–61.
[68] Raucci F, Fuet A, Pain B. In vitro generation and characterization of chicken long-term germ cells from different embryonic origins. Theriogenology 2015;84:732–42. e1-2.
[69] Deshpande G, Zhou K, Wan JY, et al. The hedgehog pathway gene shifted functions together with the hmgcr-dependent isoprenoid biosynthetic pathway to orchestrate germ cell migration. Plos Genet 2013;9:e1003720.
[70] Sun J, Ting MC, Ishii M, et al. Msx1 and Msx2 function together in the regulation of primordial germ cell migration in the mouse. Dev Biol 2016;417:11–24.